

Satellite observations reveal extreme methane leakage from a natural gas well blowout

Sudhanshu Pandey^{a,b,1}, Ritesh Gautam^c, Sander Houweling^{a,d}, Hugo Denier van der Gon^e, Pankaj Sadavarte^{a,e}, Tobias Borsdorff^a, Otto Hasekamp^a, Jochen Landgraf^a, Paul Tol^a, Tim van Kempen^a, Ruud Hoogeveen^a, Richard van Hees^a, Steven P. Hamburg^c, Joannes D. Maasakkers^a, and Ilse Aben^a

^aSRON Netherlands Institute for Space Research, 3584 CA, Utrecht, The Netherlands; ^bInstitute for Marine and Atmospheric Research Utrecht, Utrecht University, 3584 CC, Utrecht, The Netherlands; ^cEnvironmental Defense Fund, New York, NY 10010; ^dDepartment of Earth Sciences, Vrije Universiteit Amsterdam, 1081 HV, Amsterdam, The Netherlands; and ^eDepartment of Climate, Air and Sustainability, TNO, 3584 CB, Utrecht, The Netherlands

Edited by Paul B. Shepson, Stony Brook University, and accepted by Editorial Board Member Ravi R. Ravishankara November 6, 2019 (received for review May 20, 2019)

Methane emissions due to accidents in the oil and natural gas sector are very challenging to monitor, and hence are seldom considered in emission inventories and reporting. One of the main reasons is the lack of measurements during such events. Here we report the detection of large methane emissions from a gas well blowout in Ohio during February to March 2018 in the total column methane measurements from the spaceborne Tropospheric Monitoring Instrument (TROPOMI). From these data, we derive a methane emission rate of 120 ± 32 metric tons per hour. This hourly emission rate is twice that of the widely reported Aliso Canyon event in California in 2015. Assuming the detected emission represents the average rate for the 20-d blowout period, we find the total methane emission from the well blowout is comparable to one-quarter of the entire state of Ohio's reported annual oil and natural gas methane emission, or, alternatively, a substantial fraction of the annual anthropogenic methane emissions from several European countries. Our work demonstrates the strength and effectiveness of routine satellite measurements in detecting and quantifying greenhouse gas emission from unpredictable events. In this specific case, the magnitude of a relatively unknown yet extremely large accidental leakage was revealed using measurements of TROPOMI in its routine global survey, providing quantitative assessment of associated methane emissions.

methane | TROPOMI | satellite remote sensing | natural gas | well blowout

Methane (CH₄) is the second largest contributor to global warming after carbon dioxide, accounting for at least one-quarter of the present-day warming (1). This, combined with its short atmospheric lifetime of ~10 y, means reductions in CH₄ emissions can effectively reduce the rate of near-term climate warming (2). To this end, accurately quantifying CH₄ emissions from the oil and natural gas (O&G) infrastructure, one of the largest sources of anthropogenic CH₄, has been the focus of a large body of research over the past few years (3–9). Further, emissions from the natural gas supply chain impact the climate benefits of using natural gas relative to other fossil fuels. Hence, reducing CH₄ emissions is an increasing focus of the O&G industry and governments (10–13).

Recent studies indicate that O&G CH₄ emissions may be significantly underestimated or mischaracterized (6–9, 14–18). Ground and airborne measurement campaigns have built a clearer picture of these emissions, indicating US O&G emissions are 60% higher than in the US Environmental Protection Agency (EPA) emission inventories (9, 19). One of the possible causes for such a large discrepancy is suggested to be CH₄ “superemitters” linked to abnormal process conditions in the O&G infrastructure (16).

In addition to superemitters, accidental leakages in the O&G sector can result in extremely large releases of CH₄ to the atmosphere from even a single-point failure (4, 20–22). For example, 115 kilotons (kt) of natural gas, mostly consisting of CH₄, was released due to the collapse of an underground storage facility in Moss Bluff, TX, in 2004 (4, 22). The well-studied 2015 blowout

of the Aliso Canyon underground storage facility in California resulted in 97 kt of CH₄ released during a ~3.5-mo period (4). This amount of CH₄ emission is larger than the reported annual O&G emissions of most European countries (23). Such accidental CH₄ emissions usually go unquantified and unreported in emission inventories, especially when they happen in remote areas, where a large fraction of O&G facilities are located. Monitoring accidental CH₄ emissions is challenging, as it is not feasible to carry out frequent airborne or ground surveys across the entire O&G supply chain. However, space-based CH₄ measurements with global coverage have the potential to detect and quantify such large point source emission events (24).

On 15 February 2018, a gas well (39.864°N, 80.861°W) exploded in Belmont county of Ohio (<https://youtu.be/D0F450ESHP8>). The well blowout resulted in an uncontrolled venting of natural gas with a preliminary estimate of 100 million cubic feet per day (25, 26). This amount is equivalent to 80 t/h of CH₄ assuming 95% CH₄ composition at standard pressure and temperature. The CH₄ release continued for nearly 20 d until 7 March when the well was

Significance

Emissions from the fossil fuel industry are one of the major sources of atmospheric methane. Gas leakages due to accidents in the oil and gas sector can release large amounts of methane within short periods of time. Although these emissions are very challenging to monitor, satellite measurement platforms offer a promising approach by regularly scanning the entire globe. This study demonstrates this capability of satellite measurements by reporting atmospheric measurements of methane emission from a natural gas well blowout in Ohio in 2018. Assuming a constant emission rate during the whole event, we find the total methane emission from the 20-d blowout to be equivalent to a substantial fraction of the annual total anthropogenic emission of several European countries.

Author contributions: S.P., R.G., S.H., and I.A. led the study; P.T., T.K., R.H., and R.v.H. provided detailed analysis of the TROPOMI SWIR measurements and LB1 data; T.B., O.H., and J.L. provided the TROPOMI XCH₄ retrievals; S.P. analyzed the TROPOMI XCH₄ data and carried out WRF simulations; H.D.G., P.S., and J.D.M. performed the bottom-up inventory comparisons; S.P., R.G., S.H., S.P.H., and I.A. wrote the manuscript; and all authors discussed the results and commented on the manuscript.

The authors declare no competing interest.

This article is a PNAS Direct Submission. P.B.S. is a guest editor invited by the Editorial Board.

Published under the [PNAS license](#).

Data deposition: TROPOMI data are available at ftp://ftp.sron.nl/open-access-data-2/TROPOMI/tropomi/ch4/10_9/. WRF-CHEM model code is available at <https://ruc.noaa.gov/wrf/wrf-chem/>.

¹To whom correspondence may be addressed. Email: s.pandey@sron.nl.

This article contains supporting information online at <https://www.pnas.org/lookup/suppl/doi:10.1073/pnas.1908712116/-DCSupplemental>.

closed (27). Earthworks visited the blowout site on 3 March and recorded an infrared video of the gas leakage (Movie S1).

Using total column CH_4 (XCH_4) measurements from the spaceborne Tropospheric Monitoring Instrument (TROPOMI), we detected and quantified the CH_4 emission from this event. TROPOMI is onboard the Sentinel-5P satellite launched in October 2017 and provides near-daily global XCH_4 measurements at $7 \text{ km} \times 7 \text{ km}$ ground pixel resolution at nadir. Relevant details about the TROPOMI measurements are provided in *Materials and Methods*. Satellite orbits with sufficient data coverage in the region surrounding the blowout were selected from TROPOMI measurements made between 12 November 2017 and 30 July 2018. For our application, we assumed that a coverage of a quarter of the area of the blowout region (Fig. 1A) is sufficient. The TROPOMI measurements were filtered for cloud-free conditions and low aerosol content using the same criteria as described in Hu et al. (28). During this period, measurements were not readily available, as TROPOMI was in its commissioning phase and not yet fully operational. Moreover, due to persistent cloud cover in the blowout region, only orbits on 26 and 27 February met the selection threshold during the blowout episode. On 26 February (SI Appendix, Fig. S1), there were no measurements downwind of the blowout, due to cloud cover leaving the orbit unsuitable for the detection of emission from the blowout.

On 27 February, surface winds in the region were northbound at the time of TROPOMI overpass (12:35 Ohio local time, 17:35 UTC), and a significant XCH_4 enhancement downwind of the well

was observed (Fig. 1B). This enhancement extended more than 100 km downwind. The measurements during the blowout were compared with TROPOMI measurements before (Fig. 1C; November 2017) and after (Fig. 1D; April 2018) the blowout. The absence of any significant XCH_4 enhancement downwind of the well, before and after the blowout, confirms detection of the blowout emission on 27 February. SI Appendix, Fig. S2 shows a distribution of TROPOMI measurements in the blowout region during November 2017 to July 2018. On 27 February, the largest XCH_4 enhancement was detected in a measurement pixel $\sim 36 \text{ km}$ downwind of the blowout well, exceeding the median XCH_4 of all measurements in the region by 106 ± 2 parts per billion (ppb) or 6%.

In the orbits before and after the blowout, the highest XCH_4 enhancements exceed the respective medians only by 43 ± 3 ppb and 20 ± 2 ppb (Fig. 1C and D). Additionally, these enhancements are not located downwind of the blowout location, suggesting they are caused by other sources in the region. The significantly larger enhancement on 27 February (i.e., 2 to 5 times larger than those outside of the blowout period), which cannot be explained by sustained regional emissions (SI Appendix, section 5), implies large CH_4 emissions associated with gas leakage at the blowout well. Note that the measurement pixels directly over and immediately downwind of the blowout location show less pronounced enhancements than the pixels farther downwind (Fig. 1B). We elaborate on this issue in SI Appendix, section 6.

Our detection of CH_4 emission from the Ohio blowout demonstrates the potential of satellite remote sensing to provide

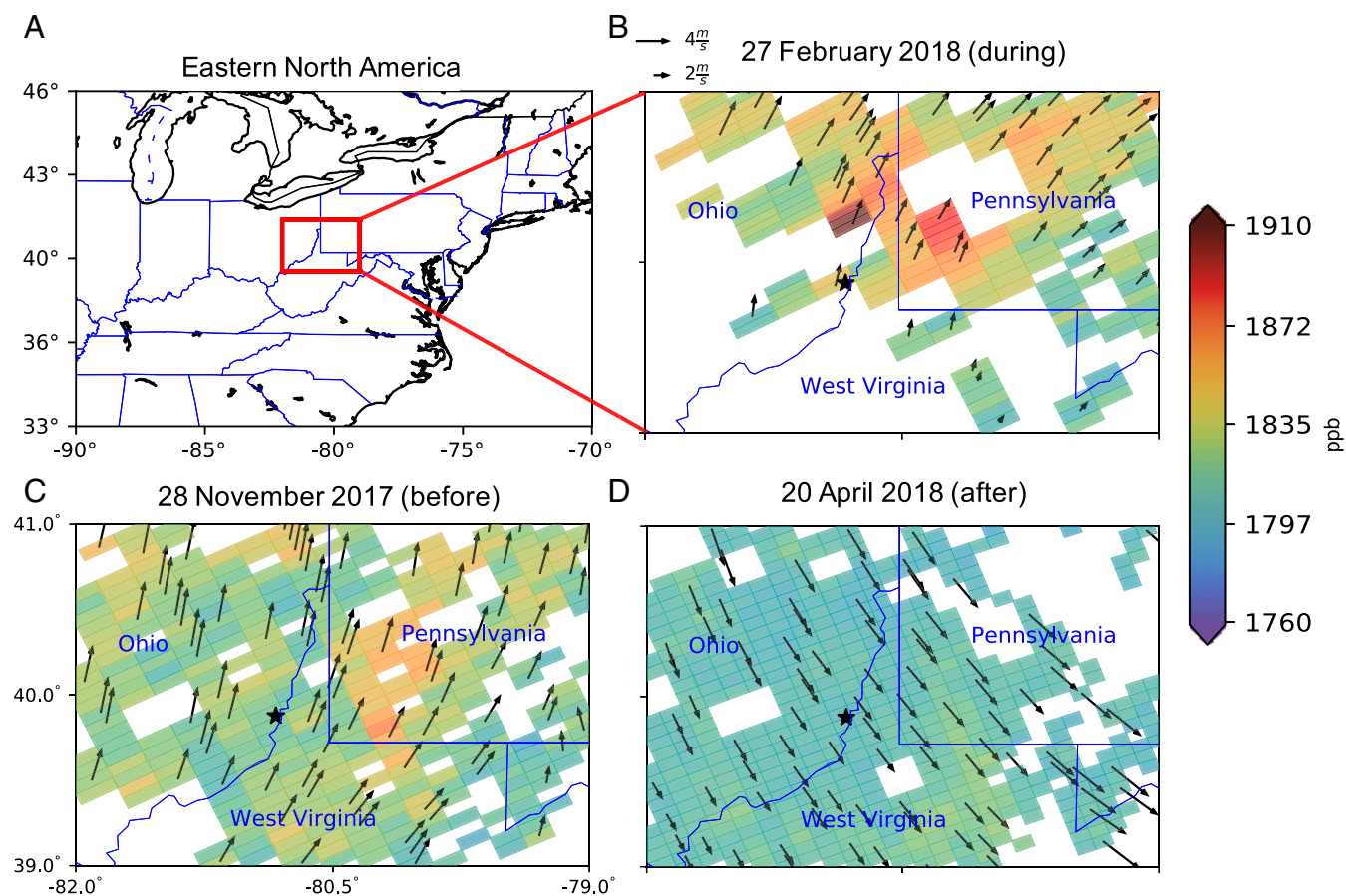


Fig. 1. TROPOMI XCH_4 measurements in the vicinity of the blowout well in Ohio. (A) Map of eastern North America showing the blowout region (79° to 82°W and 39° to 41°N) marked with a red box. (B–D) TROPOMI XCH_4 surrounding the blowout region (B) during, (C) before, and (D) after the blowout event. Respective dates are indicated on top. The location of the blowout well is marked with a star. The black arrows are wind vectors at 10 m above the surface from the ECMWF 6-hourly meteorological forecast fields.

independent measurements of accidental emissions of greenhouse gases globally. Previously, Kort et al. (29) showed that satellite measurements can identify and quantify regional CH_4 emissions using the SCIAMACHY (Scanning Imaging Absorption Spectrometer for Atmospheric Chartography) satellite instrument. However, multiyear (2003–2009) averaging of measurements was needed to characterize emissions from a high-emission region, due to SCIAMACHY's low spatial resolution ($60 \text{ km} \times 30 \text{ km}$ pixels) and precision. Thompson et al. (30) demonstrated the capability of satellite and airborne remote sensing to detect CH_4 release during the Aliso Canyon accidental leakage. However, the leakage was measured in target-mode operations of the Hyperion satellite instrument using prior knowledge about the location of the leakage, which would otherwise have escaped detection because of the limited spatial coverage of the satellite instrument.

To quantify the CH_4 emission rate of the blowout, we performed an atmospheric tracer transport simulation with a constant CH_4 release at the blowout well using the Weather Research and Forecasting (WRF) model (31). This enabled us to investigate the atmospheric dispersion of the CH_4 plume at the overpass time of TROPOMI. The setup of the WRF simulation is described in *Materials and Methods*. WRF-simulated XCH_4 at 18:00 UTC, closest to the TROPOMI overpass at 17:35 UTC on 27 February, is shown in Fig. 2A. The WRF-simulated XCH_4 , sampled at TROPOMI pixels (Fig. 2B), shows similar enhancements as seen in TROPOMI XCH_4 .

We use the mass balance approach to quantify the emission rate of the blowout. A WRF simulation of the blowout plume is scaled to match the TROPOMI-observed XCH_4 enhancement. The XCH_4 enhancement is calculated as the mean XCH_4 difference between downwind blowout-influenced and upwind background pixels shown in Fig. 2C. This leads to an emission rate of $120 \pm 32 \text{ t/h}$ (1 SD) for the blowout. *Emission Rate Quantification* describes the implementation of mass balance approach, and *SI Appendix, section 1* describes the uncertainty quantification. In addition to the mass balance method, we also use the cross-sectional flux method (15, 32), resulting in an emission rate of $130 \pm 28 \text{ t/h}$ (*SI Appendix, section 2*). The two emission rate estimates, calculated using different methods, are in close agreement. In *SI Appendix, section 5*, we assess the contribution of other anthropogenic CH_4 sources in the downwind blowout-influenced region. This contribution is less than 5% of the XCH_4 enhancement, indicating that the enhancement in the region is primarily caused by the blowout.

To assess the significance of the TROPOMI-derived emission rate from the blowout, we compare it with previously known accidental and regional emissions across the US O&G sector. The blowout emission rate appears to be significantly larger (2 times) than the peak emission rate from the Aliso Canyon leakage event (60 t/h), reported as the second largest CH_4 release of its kind in the United States (4). Further, our results indicate that the blowout in Ohio emitted more CH_4 per hour than any of the 9 O&G basins reported by Alvarez et al. (9) (Fig. 3A, *Inset*), that, in total, account for $\sim 33\%$ of US natural gas production.

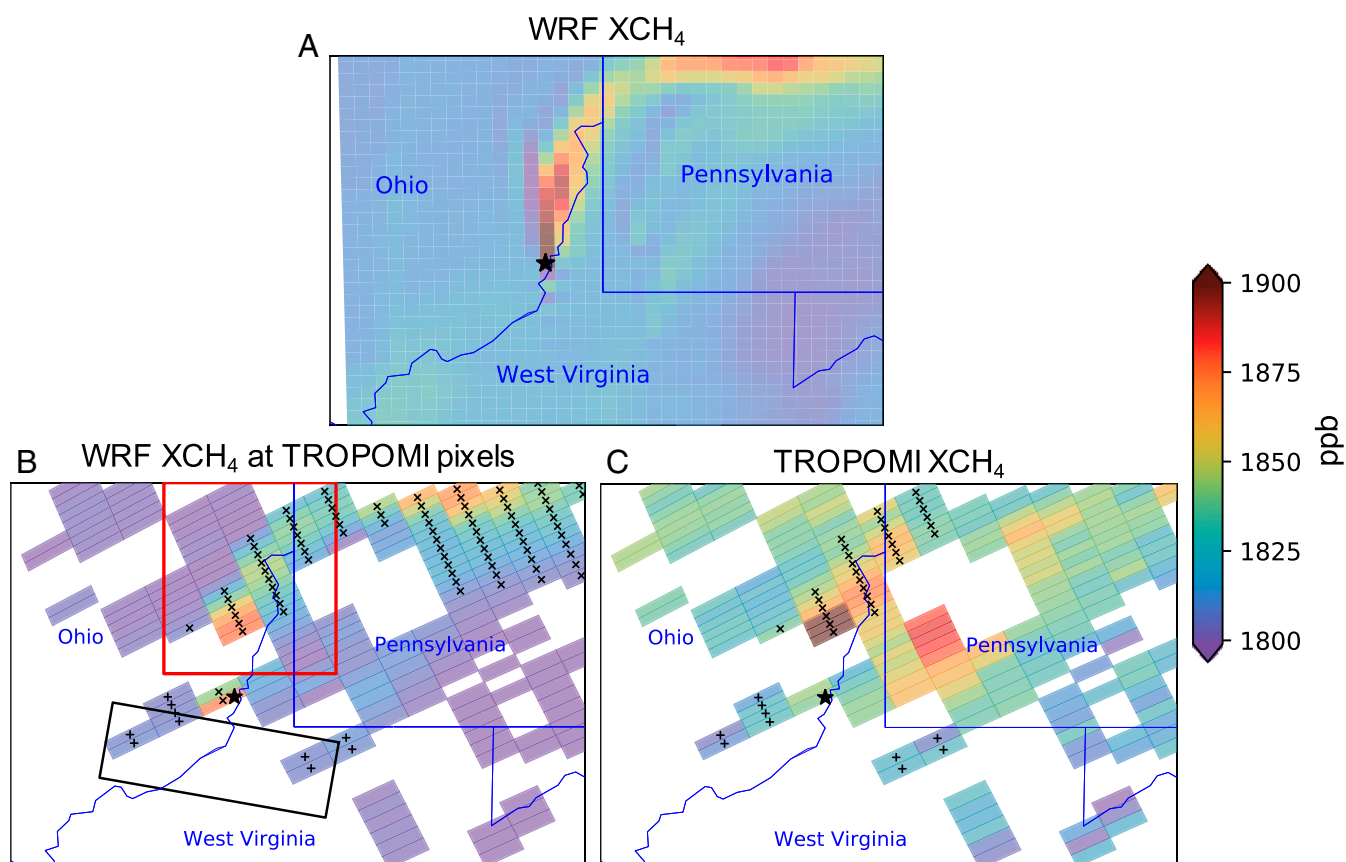


Fig. 2. Comparison of WRF-simulated and TROPOMI-observed XCH_4 . The blowout location is marked with a black star. (A) WRF-simulated column averaged mixing ratio of CH_4 (XCH_4) at 18:00 UTC on 27 February 2018 in the blowout region. (B) WRF XCH_4 sampled at TROPOMI pixels. The pixels influenced by the blowout emission are marked with crosses (influence mask; see *Emission Rate Quantification*). The rectangle south of the blowout location marks the background region. It is rotated such that its longer side is perpendicular to the local wind direction. The pixels of the background region are marked with pluses. The red box north of the blowout marks the pixels close to the blowout in downwind direction (40.0° to 41.0° latitude and -81.1° to -80.3° longitude; see *Emission Rate Quantification*). (C) TROPOMI XCH_4 at 17:35 UTC. The pixels marked with crosses in C are used in the emission quantification.

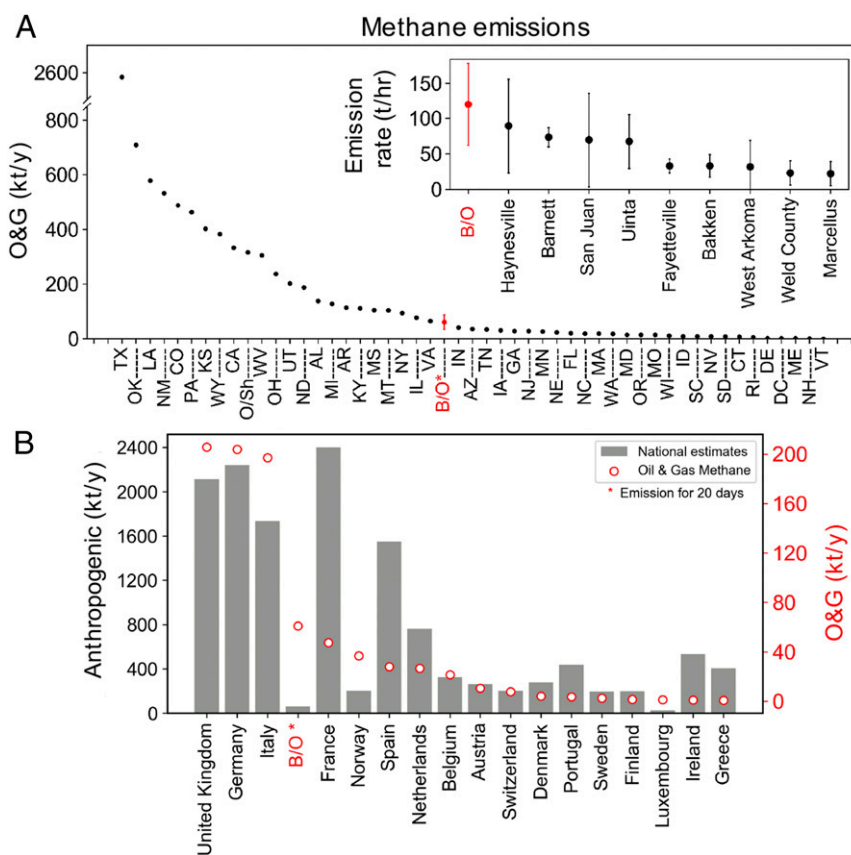


Fig. 3. Comparison of CH₄ emission from the blowout (B/O) with regional emissions. (A) Annual O&G emissions from individual states in the United States (and US offshore emissions shown by "O/Sh"), reported for year 2012, derived from the spatially disaggregated EPA gridded inventory (19). *Inset* shows the CH₄ emission rate from 9 O&G basins in the United States reported by Alvarez et al. (9), with error bars showing 95% confidence interval derived assuming a standard normal error distribution; Marcellus is reported for northeast Pennsylvania only (9). (B) Annual O&G (red circles, right-hand y axis) and total anthropogenic emissions (vertical bars, left-hand y axis) from different European Union countries (plus Switzerland and Norway) as reported to the UNFCCC (23).

TROPOMI observed the blowout emission on 27 February 2018, which was the 13th day in the blowout period, which likely does not represent the peak emission rate. Generally, the emission rate is expected to reduce linearly or exponentially due to the well pressure decreasing over time, as has previously been reported in accidental gas release episodes from Aliso Canyon in California (4) and Elgin gas platform in the North Sea (33). If this emission rate of 120 ± 32 t/h is assumed to represent the average emission rate during the blowout period, total CH₄ emission during the 20 d of the event would be 60 ± 15 kt. Note that, if there was a sustained reduction in emission rate, occurring throughout the 20-d blowout period, the total emissions will likely be larger than our estimate. Also, our uncertainty estimate is valid under the assumption that the quantified emission represents the mean of the full blowout period. Depending on the actual time dependence of the emission, the actual uncertainty could be higher. We elaborate on this in *SI Appendix, section 7*.

The total estimated blowout emission amount of 60 ± 15 kt is larger than the reported annual O&G emissions from over half of the US states individually (Fig. 3A), and equivalent to a quarter of the reported annual CH₄ emissions from the O&G sector in the entire state of Ohio (231 kt). Moreover, total emissions from this single event are equivalent to a substantial fraction of the annual anthropogenic emissions from several European countries (23) (Fig. 3B). In fact, annual O&G emissions from only 3 of the EU-15 countries (plus Switzerland and Norway) are estimated to be higher than that of the blowout. These comparisons highlight the importance of accidental emissions for regional- and national-scale

emission reporting and inventories, as the lack of incorporating such emissions can lead to significant underestimation of overall emissions.

We show detection and quantification of an accidental emission from a satellite during routine operations (i.e., without pointing the satellite to a previously known target area), which demonstrates the unique value of satellite remote sensing, and the TROPOMI instrument in particular. We provide here quantitative estimates of the magnitude of leakage from this gas well blowout in Ohio, which has not been reported in the scientific literature to date and has even received considerably less attention in the media, despite its emission rate exceeding the Aliso Canyon leakage event by a factor of 2—which was reported as the second largest accidental CH₄ release in the United States (4).

To combat climate change and build a low-carbon economy, being able to accurately monitor greenhouse gas emissions is an essential prerequisite. Our study shows how CH₄ emissions from large gas leakages due to accidents in the O&G sector can escape the greenhouse gas emission accounting system, adding a significant source of uncertainty to the annual estimates reported to the United Nations Framework Convention on Climate Change (UNFCCC). It underscores the importance of independent monitoring of greenhouse gases using atmospheric measurements. Detection and quantification of unpredictable emission poses an important challenge to the global atmospheric monitoring capacity. However, as demonstrated here, measurements from TROPOMI and other Earth-orbiting satellites offer the extended monitoring capabilities needed to tackle this problem.

Materials and Methods

TROPOMI Measurements. TROPOMI is onboard the Sentinel-5 Precursor satellite, which is in a sun-synchronous orbit at 824-km altitude (34). TROPOMI retrieves total column CH₄ (XCH₄) from Earthshine radiance measurements in the 2.3- μ m spectral range. It is a push-broom imaging spectrometer observing a 2,600-km swath and orbits the Earth in about 100 min, resulting in daily global coverage. TROPOMI has ground pixel resolution of ~ 7 km \times 7 km at nadir (with larger ground pixels toward the edges of the swath). We use the TROPOMI XCH₄ “scientific product” generated at SRON Netherlands Institute for Space Research derived using a 1-band retrieval method as described in Hu et al. (28). Only high-quality measurements, retrieved under favorable cloud-free conditions, were used. These measurements were filtered, in addition, for solar zenith angle (<70°), low viewing zenith angle (<60°), smooth topography (1 SD of surface elevation of <80 m within 5-km radius), and low aerosol load (aerosol optical thickness in 2.3- μ m band of <0.1) as in Hu et al. (28).

WRF Simulation. We used version 3.8.1 of WRF (31) and its CHEM module (35). The WRF simulation was nudged to National Centers for Environmental Prediction final analysis meteorological fields at 1° \times 1° spatial and 6-h temporal resolution. The model is run for a single uniform spatial domain (Fig. 1A) with a horizontal dimension of 59 \times 66 grid boxes of 5 km \times 5 km each centered at 80.25°W and 40.0°N, and 29 vertical eta levels. Other WRF settings are the same as used in Dekker et al. (36). WRF is run for the period of 20 February to 5 March 2018 to simulate the atmospheric transport of blowout emissions, EPA emissions, and CH₄ boundary conditions as 3 independent tracers. The blowout tracer represents constant CH₄ “point” emission of 80 t/h at the blowout well location, based on the reported natural gas flow rate of 100 million cubic feet per day (25, 26) and assuming a CH₄ fraction of 95% at standard temperature and pressure. The EPA tracer represents anthropogenic CH₄ emissions taken from EPA’s gridded national inventory of the United States (19). The boundary tracer accounts for CH₄ transport across the initial and lateral boundaries of the selected WRF model domain. These boundary conditions are taken from the European Centre for Medium-Range Weather Forecasts (ECMWF) Copernicus Atmosphere Monitoring Service near-real-time analysis (37).

At the TROPOMI overpass time on 27 February 2018, the WRF-generated wind fields are also northbound at the well location. A large plume-shaped enhancement is visible downwind of the blowout (Fig. 2A). To obtain WRF output representative of the TROPOMI XCH₄ spatial distribution, the spatially continuous WRF XCH₄ was sampled according to the TROPOMI measurement pixels (Fig. 2B). The averaging kernels of the XCH₄ retrievals were used to account for the sensitivity of the TROPOMI measurements to the vertical distribution of CH₄ in the atmosphere. A large enhancement is seen in resampled WRF XCH₄ ~ 30 km downwind of the blowout location, similar to the enhancement seen in TROPOMI XCH₄. The elongated XCH₄ enhancement plume extends to the northeast edge of the model domain.

Emission Rate Quantification. The emission rate from the blowout (Q_T) is quantified by comparing TROPOMI-observed and WRF-simulated XCH₄ enhancements,

$$Q_T = Q_W * \frac{X_T}{X_W} \quad [1]$$

where, X_T and X_W are the XCH₄ enhancements (in parts per billion) for TROPOMI and WRF, respectively. Enhancements are calculated as the

difference between the blowout-influenced XCH₄ pixels and the background pixels. To select blowout-influenced pixels downwind of the source, a Boolean mask is defined to select pixels that are influenced by the blowout and are in the vicinity of the blowout. This influence mask flags pixels that are enhanced by the blowout emission according to independent WRF-simulated XCH₄ of the blowout tracer (i.e., without XCH₄ contribution from EPA and boundary tracers). A pixel is flagged if WRF XCH₄ sampled at the TROPOMI pixel exceeds the mean retrieval precision in the considered region (= 2.2 ppb). Note that this retrieval precision only accounts for the radiance noise and no other sources of error in the XCH₄ measurements. The influence mask is indicated by crosses in Fig. 2B. To minimize the uncertainties in the WRF-simulated blowout plume, which are expected to increase with the distance from the source, we only use pixels close to the source, as indicated by the red rectangle north of the blowout location in Fig. 2B and C. The upwind background region is marked by the black rectangle in Fig. 2B, which has been rotated such that its long sides are perpendicular to the wind direction at the blowout location. The pixels within this box are marked by pluses and represent the upwind background.

Q_W (= 80 t/h) is the input emission at the blowout location in the WRF simulation. X_W is calculated as the sum of the independent boundary, blowout, and EPA tracers. EPA emissions are simulated to account for non-blowout emissions, and the boundary tracer is simulated to account for variations in XCH₄ due to elevation and variations in CH₄ transported from outside of the WRF domain. We found X_T and X_W to be 40 ppb and 27 ppb, respectively, resulting in $Q_T = 116$ t/h. After accounting for various sources of errors (SI Appendix, section 1), a final emission rate of 120 ± 32 t/h is derived.

Data and Materials Availability. TROPOMI data are available at ftp://ftp.sron.nl/open-access-data-2/TROPOMI/tropomi/ch4/10_9/. WRF-CHEM model code is available at <https://ruc.noaa.gov/wrf/wrf-chem/>.

ACKNOWLEDGMENTS. We thank the team that has realized the TROPOMI instrument, consisting of the partnership between Airbus Defence and Space Netherlands, Royal Netherlands Meteorological Institute (KNMI), SRON Netherlands Institute for Space Research (TNO), and Netherlands Organisation for Applied Scientific Research (TNO), Netherlands Space Office (NSO), and European Space Agency. This research contains modified Copernicus Sentinel data 2017 and 2018. The methane data processing was carried out on the Dutch national e-infrastructure with the support of SURF Cooperative. We would also like to thank David Lyon, Environmental Defense Fund, for stimulating discussions regarding the well blowout in Ohio and US O&G emissions. We also thank Anthony J. Marchese, Colorado State University, for sharing with us gas flow rate sensitivity calculations representative of the well blowout event. Earthworks is kindly acknowledged for making available the videos on the blowout event. Support for R.G. and S.P.H. was provided by the Robertson Foundation. This research is supported through the GALEs (Gas Leaks from Space) project (Grant 15597) by the Dutch Technology Foundation, which is part of the Netherlands Organisation for Scientific Research (NWO), and is partly funded by Ministry of Economic Affairs, The Netherlands. T.B., P.T., and T.K. are funded by the TROPOMI national program from the NSO.

1. G. Myhre et al., “Anthropogenic and natural radiative forcing” in *Climate Change 2013: The Physical Science Basis. Contribution of Working Group I to the Fifth Assessment Report of the Intergovernmental Panel on Climate Change*, T. F. Stocker et al., Eds. (Cambridge University Press, Cambridge, United Kingdom, 2013), pp. 659–740.
2. J. K. Shoemaker, D. P. Schrag, M. J. Molina, V. Ramanathan, Climate change. What role for short-lived climate pollutants in mitigation policy? *Science* **342**, 1323–1324 (2013).
3. A. J. Marchese et al., Methane emissions from United States natural gas gathering and processing. *Environ. Sci. Technol.* **49**, 10718–10727 (2015).
4. S. Conley et al., Methane emissions from the 2015 Aliso Canyon blowout in Los Angeles, CA. *Science* **351**, 1317–1320 (2016).
5. R. A. Alvarez, S. W. Pacala, J. J. Winebrake, W. L. Chameides, S. P. Hamburg, Greater focus needed on methane leakage from natural gas infrastructure. *Proc. Natl. Acad. Sci. U.S.A.* **109**, 6435–6440 (2012).
6. A. R. Brandt et al., Energy and environment. Methane leaks from North American natural gas systems. *Science* **343**, 733–735 (2014).
7. D. T. Allen et al., Measurements of methane emissions at natural gas production sites in the United States. *Proc. Natl. Acad. Sci. U.S.A.* **110**, 17768–17773 (2013).
8. T. L. Vaughn et al., Temporal variability largely explains top-down/bottom-up difference in methane emission estimates from a natural gas production region. *Proc. Natl. Acad. Sci. U.S.A.* **115**, 11712–11717 (2018).
9. R. A. Alvarez et al., Assessment of methane emissions from the U.S. oil and gas supply chain. *Science* **361**, 186–188 (2018).
10. United States Environmental Protection Agency, Global Methane Initiative. <https://www.epa.gov/gmi>. Accessed 18 February 2019.
11. Oil and Gas Climate Initiative, Announcing OGCI climate investments. <https://oilandgasclimateinitiative.com/announcing-ogci-climate-investments/>. Accessed 18 February 2019.
12. The White House Office of the Press Secretary, U.S.–Canada joint statement on climate, energy, and Arctic leadership. <https://pm.gc.ca/en/news/statements/2016/03/10/us-canada-joint-statement-climate-energy-and-arctic-leadership>. Accessed 18 August 2019.
13. California Legislative Information, SB-1383, “Short-lived climate pollutants: Methane emissions: Dairy and livestock: Organic waste: Landfills, California legislative information. https://leginfo.ca.gov/faces/billNavClient.xhtml?bill_id=2015201605B1383. Accessed 15 February 2019.
14. S. Schwietzke et al., Improved mechanistic understanding of natural gas methane emissions from spatially resolved aircraft measurements. *Environ. Sci. Technol.* **51**, 7286–7294 (2017).
15. C. Frankenberg et al., Airborne methane remote measurements reveal heavy-tail flux distribution in Four Corners region. *Proc. Natl. Acad. Sci. U.S.A.* **113**, 9734–9739 (2016).
16. D. Zavala-Araiza et al., Super-emitters in natural gas infrastructure are caused by abnormal process conditions. *Nat. Commun.* **8**, 14012 (2017).
17. T. I. Yacovitch, Methane emissions in The Netherlands: The Groningen field. *Elem. Sci. Anth.* **6**, 57 (2018).
18. S. Baray et al., Quantification of methane sources in the Athabasca Oil Sands Region of Alberta by aircraft mass balance. *Atmos. Chem. Phys.* **18**, 7361–7378 (2018).
19. J. D. Maasakkers et al., Gridded national inventory of U.S. methane emissions. *Environ. Sci. Technol.* **50**, 13123–13133 (2016).

20. Marcellus Drilling News, Triad Hunter well blowout in Monroe County, OH—No one injured. <https://marcellusdrilling.com/2014/12/triad-hunter-well-blowout-in-monroe-county-oh-no-one-injured/>. Accessed 2 September 2019.
21. FrackCheckWV.net, Blast and fire at blue racer processing plant in Ohio valley kills worker. <http://www.frackcheckwv.net/2014/11/14/blast-and-fire-at-blue-racer-processing-plant-in-ohio-valley-kills-worker/>. Accessed 2 September 2019.
22. Fox News, Second gas blast rocks Texas facility. <https://www.foxnews.com/story/second-gas-blast-rocks-texas-facility>. Accessed 2 September 2019.
23. United Nations Framework Convention on Climate Change, National inventory reports 2017. <https://unfccc.int/process-and-meetings/transparency-and-reporting/reporting-and-review-under-the-convention/greenhouse-gas-inventories-annex-i-parties/submissions/national-inventory-submissions-2017>. Accessed 2 September 2019.
24. D. J. Jacob *et al.*, Satellite observations of atmospheric methane and their value for quantifying methane emissions. *Atmos. Chem. Phys.* **16**, 14371–14396 (2016).
25. United States Environmental Protection Agency, EPA pollution situation report. https://www.fractracker.org/a5ej20sjfwe/wp-content/uploads/2018/03/XTOPowhatenPoint_polrep_1.pdf. Accessed 2 February 2019.
26. United States Environmental Protection Agency, EPA pollution situation report. https://www.fractracker.org/a5ej20sjfwe/wp-content/uploads/2018/03/XTOPowhatenPoint_polrep_2.pdf. Accessed 2 February 2019.
27. S. DiSavino, K. Palmer, Exxon's XTO caps leaking Ohio gas well, 20 days after blowout. *Reuters* (2018). <https://www.reuters.com/article/us-exxon-xto-natgas-ohio/exxon-xto-caps-leaking-ohio-gas-well-20-days-after-blowout-idUSKCN1GJ355>. Accessed 2 February 2019.
28. H. Hu *et al.*, Toward global mapping of methane with TROPOMI: First results and intersatellite comparison to GOSAT. *Geophys. Res. Lett.* **45**, 3682–3689 (2018).
29. E. A. Kort *et al.*, Four Corners: The largest US methane anomaly viewed from space. *Geophys. Res. Lett.* **41**, 6898–6903 (2014).
30. D. R. Thompson *et al.*, Space-based remote imaging spectroscopy of the Aliso Canyon CH₄ superemitter. *Geophys. Res. Lett.* **43**, 6571–6578 (2016).
31. W. C. Skamarock *et al.*, "A description of the Advanced Research WRF Version 3" (Tech. Rep. NCAR/TN-475+STR, National Center for Atmospheric Research, 2008).
32. D. J. Varon *et al.*, Quantifying methane point sources from fine-scale satellite observations of atmospheric methane plumes. *Atmos. Meas. Tech.* **11**, 5673–5686 (2018).
33. J. D. Lee *et al.*, Flow rate and source reservoir identification from airborne chemical sampling of the uncontrolled Elgin platform gas release. *Atmos. Meas. Tech.* **11**, 1725–1739 (2018).
34. J. P. Veefkind *et al.*, TROPOMI on the ESA sentinel-5 precursor: A GMES mission for global observations of the atmospheric composition for climate, air quality and ozone layer applications. *Remote Sens. Environ.* **120**, 70–83 (2012).
35. G. A. Grell, S. R. Freitas, A scale and aerosol aware stochastic convective parameterization for weather and air quality modeling. *Atmos. Chem. Phys.* **14**, 5233–5250 (2014).
36. I. N. Dekker *et al.*, Quantification of CO emissions from the city of Madrid using MOPITT satellite retrievals and WRF simulations. *Atmos. Chem. Phys.* **17**, 14675–14694 (2017).
37. E. N. Koffi, P. Bergamaschi, "Evaluation of Copernicus Atmosphere Monitoring Service methane products" (Tech. Rep. EUR 29349 EN, European Commission Joint Research Centre, 2018).